ELSEVIER

Journal of Immunological Methods 246 (2000) 79–90

JIM
Journal of
Immunological Methods

www.elsevier.nl/locate/jim

Rapid quantitation of proinflammatory and chemoattractant cytokine expression in small tissue samples and monocyte-derived dendritic cells: validation of a new real-time RT-PCR technology

Volker Blaschke[a,*], Kristian Reich[a], Sabine Blaschke[b], Sabine Zipprich[a], Christine Neumann[a]

[a]*Department of Dermatology, von-Siebold-Str. 3, D-37075 Goettingen, Germany*
[b]*Department of Nephrology, Georg-August-University, Goettingen, Germany*

Received 3 April 2000; received in revised form 21 August 2000; accepted 11 September 2000

Abstract

The analysis of cytokine profiles plays a central part in the characterization of disease-related inflammatory pathways and the identification of functional properties of immune cell subpopulations. Because tissue biopsy samples are too small to allow the detection of cytokine protein, the detection of mRNA by RT-PCR analysis is often used to investigate the cytokine milieu in inflammatory lesions. RT-PCR itself is a qualitative method, indicating the presence or absence of specific transcripts. With the use of internal or external standards it may also serve as a quantitative method. The most widely accepted method is quantitative competitive RT-PCR, based on internal shortened standards. Recently, online real-time PCR has been introduced (LightCycler®), which allows quantitation in less than 30 min. Here, we have tested its use for the analysis of cytokine gene expression in different experimental in vitro and ex vivo settings. First, we compared quantitative competitive RT-PCR with real-time RT-PCR in the quantitation of transcription levels of the $CD4^+$ cell-specific chemoattractant Interleukin-16 during the maturation of monocyte-derived dendritic cells, and found a good correlation between both methods. Second, differences in the amounts of IL-16 mRNA in synovial tissue from patients with rheumatoid arthritis and osteoarthritis as assessed by real-time RT-PCR paralleled differences in the level of IL-16 protein in the synovial fluid. Finally, we employed real-time RT-PCR to study the cutaneous expression of several cytokines during experimental immunomodulatory therapy of psoriasis by Interleukin-10, and demonstrate that the technique is suitable for pharmacogenomic monitoring. In summary, real-time RT-PCR is a sensitive and rapid tool for quantifying mRNA expression even with small quantities of tissue. The results obtained do not differ from those generated by quantitative competitive RT-PCR.

Keywords: Quantitative competitive RT-PCR; Real-time RT-PCR; LightCycler®; Interleukin-16; Interleukin-10 therapy; Rheumatoid arthritis; Psoriasis; Dendritic cell

Abbreviations: FCS, fetal calf serum; IFN-γ, interferon-γ; OA, osteoarthritis; PCR, polymerase chain reaction; PUVA, psoralene UVA; RA, rheumatoid arthritis; RT, reverse transcription; TNFα, tumour necrosis factor α

*Corresponding author. Tel.: +49-551-39-6410; fax: +49-551-39-8413.
E-mail address: vblasch@gwdg.de (V. Blaschke).

0022-1759/00/$ – see front matter
PII: S0022-1759(00)00304-5

1. Introduction

Recent studies have shown that several chronic inflammatory disorders are associated with specific changes in the balance between pro- and anti-inflammatory cytokines in affected compared to normal tissue. For example, in two types of chronic skin inflammation, psoriatic lesions are characterized by a preferential expression of Th1-type cytokines (Uyemura et al., 1993; Schlaak et al., 1994), whereas in early lesions of atopic dermatitis Th2-type cytokines have been observed (Sager et al., 1992; Neumann et al., 1996). However, the characterization of cytokine profiles is often hampered by the fact that only small amounts of tissue (typically punch biopsies) are available for investigation. Hence, quantitative investigations on the protein level are rarely undertaken, as detection methods such as ELISA are not sensitive enough and permit the analysis of only a limited number of factors from one sample. Therefore, expression analysis is often performed at the mRNA level by Northern blot analysis or RT-PCR. While Northern blot analysis requires considerable amounts of tissue material, RT-PCR is a highly sensitive method allowing the detection of mRNA transcripts from small quantities due to the exponential amplification process. RT-PCR is a qualitative method indicating the presence or absence of specific transcripts. Due to the exponential amplification and inter-sample variations in amplification efficiency, the amount of PCR product obtained does not provide a valid measure for the amount of a specific transcript present within the sample (Gilliland et al., 1990). By using external or internal standards, the amplification process can be controlled, allowing RT-PCR to be used quantitatively. The currently preferred method is quantitative competitive RT-PCR, where shortened constructs (internal standards) compete for the same sequence-specific primer pairs and are co-amplified in the same reaction tube (Gilliland et al., 1990). The wild-type and internal standard PCR products can afterwards be separated, e.g., by agarose gel electrophoresis, and subsequently quantified. To control for inter-sample variations, cytokine expression levels are standardized for a housekeeping gene, usually β-actin or GAPDH. This method is accurate, but tedious and time consuming. Recently, real-time PCR has become available, using either labelled sequence-specific probes (e.g., TaqMan®, Heid et al., 1996) or a fluorescent dye (e.g., SYBR Green, ethidium bromide, Higuchi et al., 1992) to monitor the formation of PCR products. However, since competitive and real-time RT-PCR use different approaches for quantitation (internal versus external standards), it has been unclear whether both techniques give identical results when quantifying cytokine expression. Therefore, in this study we have tested both methods for the quantitation of the $CD4^+$ specific chemoattractant IL-16 during the maturation of monocyte-derived dendritic cells. Next, we investigated whether real-time RT-PCR could be used to quantify cytokine gene expression in small tissue samples. In patients with rheumatoid arthritis we compared IL-16 mRNA expression levels in synovial membrane tissue with protein expression in synovial fluid. Third, we used real-time RT-PCR to analyse the effects of subcutaneous IL-10 therapy on cutaneous proinflammatory cytokine pathways in psoriasis (Reich et al., 1998). We found that (i) quantitative competitive and real-time RT-PCR gave comparable results when quantitating IL-16 mRNA levels in monocyte-derived dendritic cells; (ii) the results of IL-16 mRNA quantitation by real-time RT-PCR from synovial membrane correlated well with IL-16 protein levels in the affected joints of rheumatoid arthritis and osteoarthritis patients; and (iii) real-time RT-PCR allowed the simultaneous detection of multiple disease-related cytokines in psoriasis and could be used for pharmacogenomic monitoring of experimental immunomodulatory therapy.

2. Materials and methods

2.1. Generation of dendritic cells

Dendritic cells were generated according to a modified protocol as previously described (Reich et al., 1999). Briefly, $CD14^+$ (purity $>85\%$) cells were positively selected from the peripheral blood mononuclear cells of healthy volunteers ($n=3$). Immature dendritic cells were obtained by incubation for 5 days in RPMI 1640/5% FCS, supplemented with 50 ng/ml rhIL-4 (Pharma Biotechnologie, Hanover, Germany) and 50 ng/ml rhGM-CSF (kindly pro-

vided by Schering-Plough Research Institute, Kenilworth, NJ, USA). Maturation of dendritic cells was induced by additional culture with 100 ng/ml TNFα (Pharma) and 50% (v/v) monocyte conditioned medium (Romani et al., 1996) for 3 days (Palucka et al., 1998). On day 8, mature dendritic cells were resuspended in medium/FCS and stimulated with TNFα (100 ng/ml) and IL-1β (10 ng/ml, Strathmann Biotech, Hanover, Germany) or TNFα, IL-1β and IL-10 (10 ng/ml, Strathmann). During culture, cells were harvested for RNA extraction on days 0, 2, 5, 7, 8 (before stimulation and 6 h after the addition of stimuli) and day 9. All donors in this study gave informed consent after the nature and possible consequences of the study had been fully explained.

2.2. Psoriasis patients and IL-10 therapy

Fourteen patients with chronic plaque psoriasis who had not received systemic immunosuppressive therapy including PUVA for at least 4 weeks or specific topical treatment for at least 2 weeks before study entry, were treated with rhIL-10 (4 μg/kg body weight, ESSEX Pharma, Munich, Germany) subcutaneously as previously described (Reich et al., 1998). The clinical response to therapy was recorded as changes in the psoriasis activity and severity index (PASI) every week. Punch biopsies were obtained from the same marker plaque before and after 42 days of therapy and snap frozen in liquid nitrogen. Control biopsies were obtained from healthy volunteers ($n=5$).

2.3. Synovial samples

Synovial fluid was collected from patients with RA ($n=15$) or OA ($n=15$). Synovial membrane tissue (RA, $n=25$; OA, $n=10$) was obtained from patients undergoing synovectomy or arthroplasty.

2.4. ELISA procedure for IL-16

IL-16 was detected in synovial fluid by a solid-phase sandwich ELISA (Biosource, Ratingen, Germany) according to the instructions of the manufacturer. Fifty μl of sample material were used per well, and values were determined in duplicate. The sensitivity of the assay was 5 pg/ml.

2.5. RNA extraction and cDNA synthesis

Total RNA was prepared (RNeasy, Qiagen, Hilden, Germany), according to the instructions of the manufacturer, from synovial membrane, harvested dendritic cells ($0.5–1\times10^6$ cells) and cryostat sections (30×20 μm) from punch biopsies. After a DNAse digestion step (FPLC-pure DNAse I, Pharmacia, Freiburg, Germany), reverse transcription (Superscript II, Gibco, Eggenstein, Germany) was performed as previously described (Blaschke et al., 1999).

2.6. Generation of internal standards

Internal standards were generated as previously described (Blaschke et al., 1996, 1999). Briefly, the β-actin F/R (Genbank accession number X00351, β-actin F 5′→3′: CCCAGCCATGTACGTTGCTAT; β-actin R 5′→3′: GGGTGGCTTTTAGGATGGCAA, product size, 1047 bp, all oligonucleotide primers by MWG, Ebersberg, Germany) and IL-16 F/R (M90391, IL-16 F: CGAAGACTCAGCTGCAAAT; IL-16 R: GCCAGGCATGAATGTCATA, 1223 bp) PCR products were cloned into the *Sma*I restriction site of the transcription vector pBluescript (Stratagene, Heidelberg, Germany). Fragments of 224 bp (*Sau*I, *Ppu*MI) and 285 bp (*Bal*I, *Cel*II) were removed from the constructs by double restriction enzyme digestion, respectively. Afterwards, the free 5′- and 3′-ends were blunted by the Klenow fragment (Pharmacia), religated and recloned (now termed 'internal standards'). They were then linearized by restriction enzyme digestion with *Bam*HI in the polylinker region, quantified by densitometric comparison to λ-DNA/*Hin*dIII fragments (Gibco) and 10-fold dilution series were prepared in water. All PCR products used in this study were identified by cycle sequencing.

2.7. Quantitative competitive PCR

Two-fold dilution series starting with 2 μl of cDNA in 11 μl of water were prepared and 5-μl aliquots were added to PCR reaction mixes con-

taining a constant known amount of the internal standard. After PCR, agarose gel electrophoresis was performed in the presence of ethidium bromide and the upper (representing wild-type cDNA) and lower (internal standard) bands were quantified by densitometry. After correcting for PCR product size, the ratios of the corresponding bands from the PCR reaction were used to quantify the molar amounts of β-actin or IL-16 cDNA molecules in the cDNA sample. Values were determined in duplicate. For each sample, the ratio of the molar amounts of IL-16 and β-actin per μl cDNA was calculated.

2.8. Generation of external standards for real-time RT-PCR

Real-time RT-PCR on the LightCycler® (Roche Diagnostics, Mannheim, Germany) was performed in a total volume of 20 μl in the presence of 2 μl of 10× reaction buffer (Taq polymerase, dNTPs, $MgCl_2$, SYBR Green, Roche Diagnostics), and 2 μl of cDNA (or water as negative control, which was always included). $MgCl_2$ was added to a final concentration of 4 mM, and 11.25 pmol of each oligonucleotide primer (Actin-LF: CCCAAGGCCAACCGCGAGAAGAT, product size, 219 bp; Actin-LR: GTCCCGGCCAGCCAGGTCCAG; IL16-LF: AAGGGGCATCTCCAACATCATCAT, 332 bp; IL16-LR: CTCCTGCCAAGCTGAACCCAAGAC; IL8-LF: CAGTTTTGCCAAGGAGTGCTAA, Genbank acc. no. X02910, 513 bp; IL8-LR: CCCGTGCAATATCTAGGAAAATC; TNFα-LF: GGCTCCAGGCGGTGCTTGTTC, M28130, 409 bp; TNFα-LR: AGACGGCGATGCGGCTGATG; CXCR2-LF: GCCCTGCCTGTCTTACTTTTC, M73969, 509 bp; CXCR2-LR: TTGGCCAGCCTGATTTTCTTTC; IFNγ-LF: TTTGGGTTCTCTTGGCTGTTACT, M29383, 418 bp; IFNγ-LR: CCTTTTTCGCTTCCCTCTTTT) were added. Real-time PCR was performed in glass capillaries with an initial denaturation step of 30 s at 95°C, followed by 40 cycles of 0 s at 95°C, 5 s annealing temperature (β-actin, 66°C; IFNγ, 59°C; TNFα, 67°C; CXCR2, 58°C; IL-8, 55°C; IL-16, 62°C) and (product length (bp)/25) s 72°C. At the end of each cycle, the fluorescence emitted by the SYBR Green was measured. After completion of the cycling process, samples were subjected to a temperature ramp (from 5°C above annealing temperature to 95°C at 2°C/s) with continuous fluorescence monitoring for melting curve analysis. Samples were loaded on an agarose gel, excised, quantified by densitometric comparison to λ-DNA/*Hin*dIII fragments (Gibco) and 10-fold dilution series prepared in water, ranging from 10 amol/μl to 0.0001 amol/μl (representing 6×10^6 to 60 copies/μl). For each PCR product, apart from primer-dimers, a single narrow peak was obtained by melting curve analysis at the specific melting temperature and only a single band of the predicted size was observed by agarose gel electrophoresis, indicating specific amplification without significant byproducts. Due to their high dilution factors, standard concentrations in the dilution series could not be measured directly. However, the fidelity of the dilution process could be assessed as a standard curve was generated (see below). By this method, the dilution series of the internal standards were also assessed after appropriate adaptation of the cycling parameters.

2.9. Quantitation of cDNA by real-time RT-PCR

From the melting curve, melting temperatures of the primer-dimer product and the specific PCR product were obtained. To exclude primer-dimer artefacts, fluorescence was not measured at the end of the extension step, but a separate detection step was added (2 s) at a temperature (β-actin, 87°C; IFNγ, 80°C; TNFα, 88°C; IL-8, 80°C; IL-16, 83°C; CXCR2, 85°C) above the melting point of primer-dimers and below the melting point of the specific PCR product. From the external standards, a calibration curve was automatically generated. Samples (determined in duplicate) were quantified accordingly (LightCycler® analysis software, version 3.39). As with quantitative competitive RT-PCR, samples were standardized for β-actin.

2.10. Statistics

All data groups were tested for Gaussian distribution. Statistical analysis was by the paired or unpaired *t*-test when applicable. Correlation between variables was analysed by Spearman's correlation coefficient. Variables are described by

mean±standard deviation (S.D.) or by median and range. Two-tailed P values <0.05 were considered as statistically significant. Statistical analysis was performed using the prism 2.01 software (GraphPad, San Diego, CA, USA).

3. Results

3.1. Quantitation of IL-16 production during maturation of dendritic cells by quantitative competitive RT-PCR

When wild-type cDNA and internal standard were co-amplified in the same tube, both competed for the binding of oligonucleotide primers according to their molar ratio, resulting in two distinct bands as observed by gel electrophoresis (Fig. 1). Bands were quantified by densitometry. After correcting for product size, the densitometric ratio of the corresponding bands was calculated for each lane. Given the amount of internal standard used for PCR and the dilution factor of the cDNA, the amount of IL-16 cDNA present in the sample could be calculated from each lane. Typically, four of the five lanes were suitable for analysis and were averaged. To allow for the comparison of different samples, results were standardized for β-actin. On day 0, there was a substantial expression of IL-16 in purified monocytes, which was markedly reduced on day 2. During dendritic cell maturation, IL-16 expression peaked in immature day 5 dendritic cells and declined with final maturation (Fig. 2).

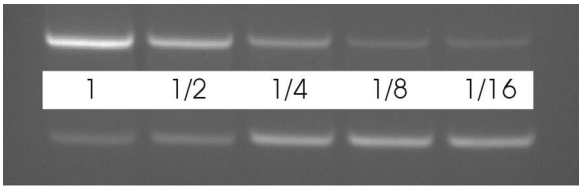

Fig. 1. Example of quantitative competitive RT-PCR. Two-fold dilution series of cDNA (1–1/16, upper bands) were coamplified with constant amounts of internal standard (lower bands). Band intensities were evaluated by densitometry and the ratio obtained from the lanes (typically four of five lanes were suitable) was used to calculate copy numbers.

3.2. Quantitation of IL-16 in dendritic cell culture by real-time RT-PCR

Fluorescence in the capillary increased with PCR product formation in a linear fashion, although signals were found to arise not only from the specific PCR product, but also from primer-dimer products. Therefore, it was important to measure the specific fluorescence at a temperature above the melting temperature of the primer-dimer product, i.e., a temperature at which primer-dimers had completely melted into single strands. The melting temperature of primer-dimer products could be determined from the negative control sample, and similarly the specific target melting temperature could be obtained (Fig. 3A). Typically, melting temperatures of primer–dimer and specific target products were at least 5°C apart. Using an intermediate temperature for quantitation, no specific fluorescence could be detected in the negative control (Fig. 3B–D). The amount of standard was inversely proportional to the number of amplification cycles necessary to detect a significant fluorescent signal above background (threshold cycle, Fig. 3C). For data analysis, the fit-point method was used to manually set the threshold between background and significant fluorescence. Given the small numbers of target copies within the cDNA samples, this method proved superior to the second-derivative method offered by the analysis software. A standard curve was generated from plotting external standard concentrations against threshold cycle (Fig. 3D). The amount of target copies in the sample was calculated from the sample threshold cycle as compared to the standard curve. All samples were determined in duplicate, and variations were typically within 10%.

3.3. Correlation of quantitative competitive PCR and real-time RT-PCR

The results obtained by quantitative competitive RT-PCR and real-time RT-PCR for IL-16 gene expression during dendritic cell maturation (Fig. 2A,B) and after stimulation of mature dendritic cells

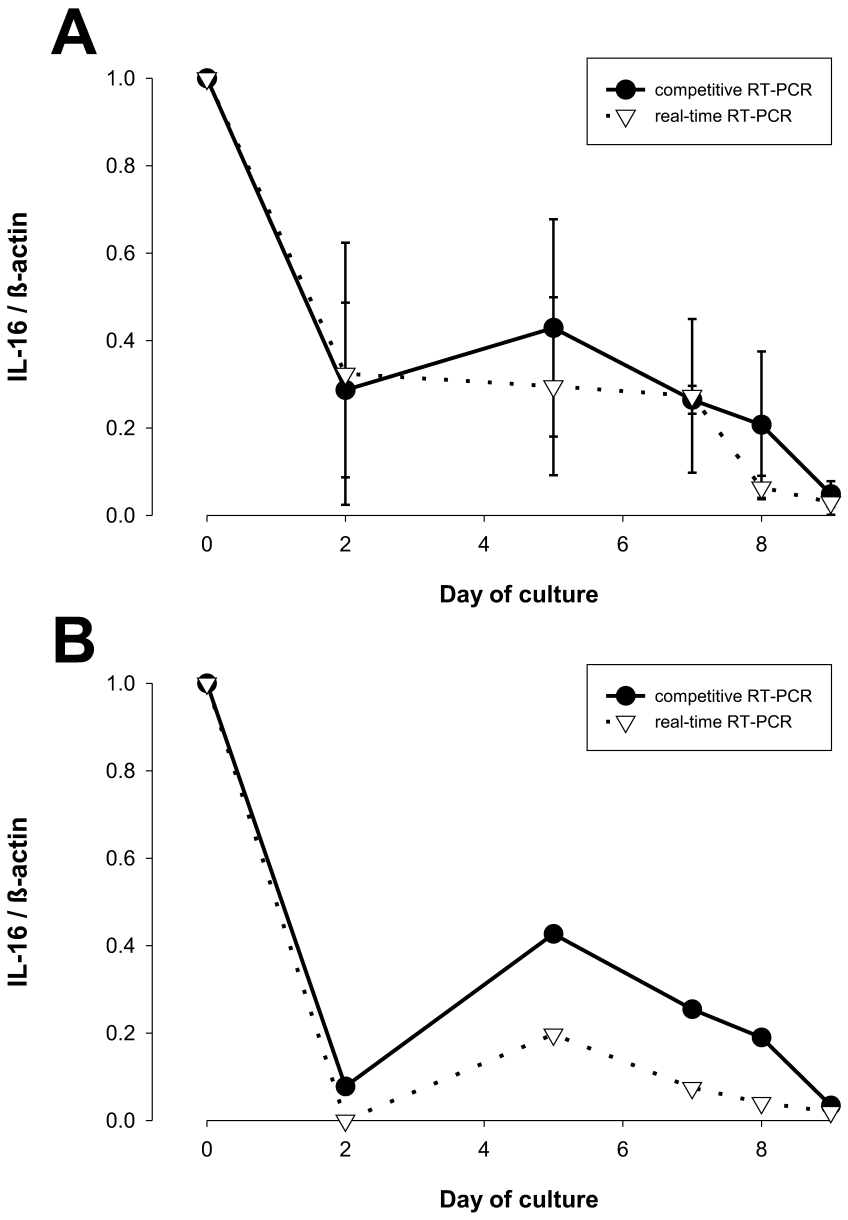

Fig. 2. IL-16 mRNA expression during dendritic cell maturation. Expression of IL-16 mRNA ($n=3$) was quantified by competitive quantitative RT-PCR and real-time RT-PCR. Results were standardized for day 0. (A) Results did not differ significantly between both methods (mean±S.D.). (B) A single, typical time course is shown.

with proinflammatory cytokines (data not shown) were similar. Thus, in a total of 27 samples quantified in parallel by both methods, we found a good correlation between both methods (Spearman $r=0.72$, $P<0.0001$).

3.4. IL-16 expression is increased in rheumatoid arthritis as compared to osteoarthritis

In synovial fluid from RA patients, IL-16 protein was significantly increased when compared to the

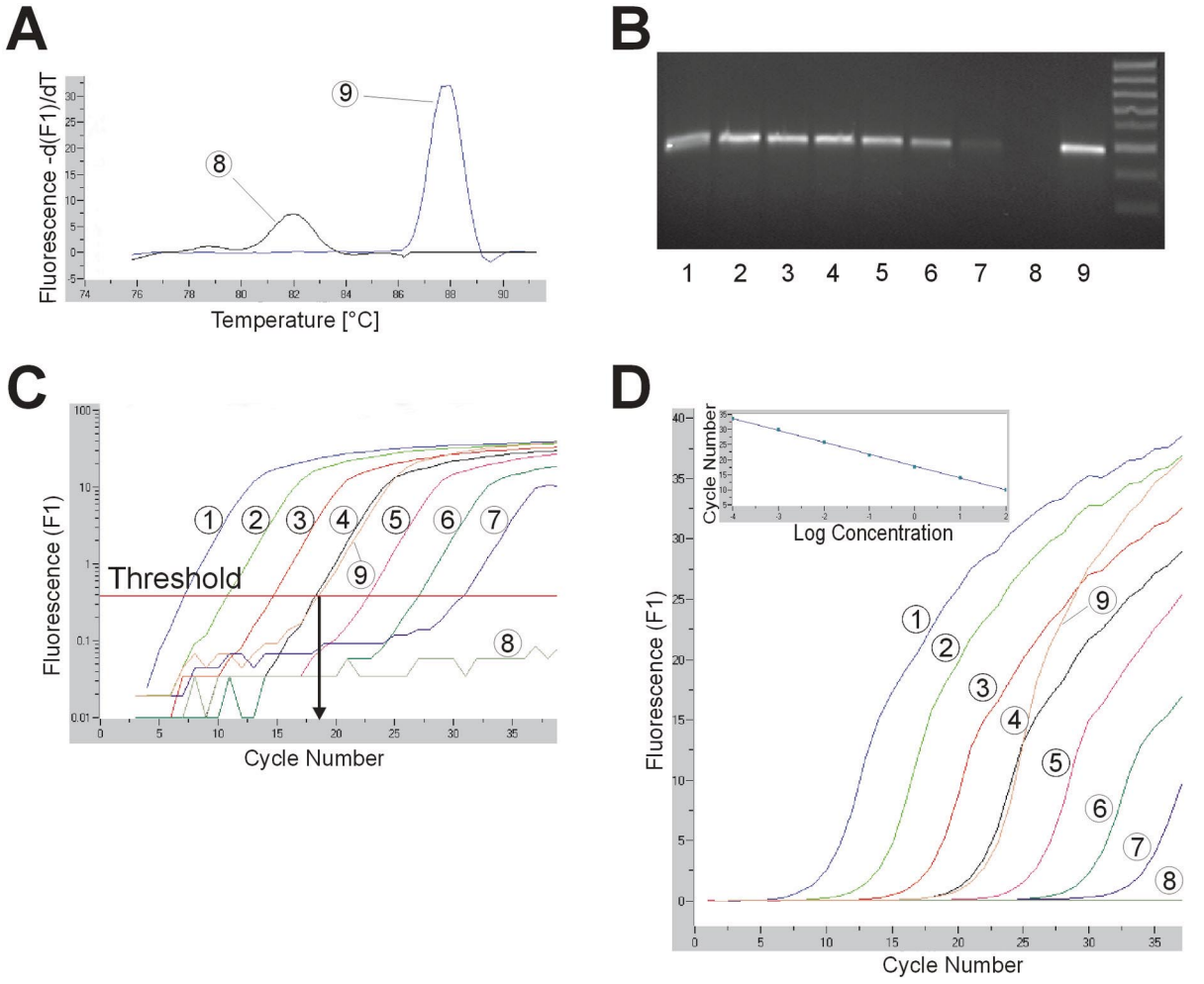

Fig. 3. Quantitation of CXCR2 by real-time RT-PCR. (A) Melting temperatures for the primer-dimer product (82°C, negative control, sample 8) and the specific target product (88°C) were determined in order to obtain the optimal temperature for fluorescence detection (85°C). (B) Ten-fold dilution series ranging from 100 amol/μl (sample 1) to 0.0001 amol/μl (sample 7), a negative control (sample 8) and a test sample (9) were subjected to real-time RT-PCR. By agarose gel electrophoresis, a single specific band was observed. (C) The threshold was set to a fluorescence intensity where all samples gave a detectable specific signal. The threshold cycle is defined by the point where sample fluorescence crosses the threshold (arrow). (D) A standard curve is generated (insert), allowing the test sample concentration to be determined. It is noteworthy that according to their respective threshold cycles, samples 4 and 9 contain similar amounts of target copies. From cycle 25 onwards, their specific fluorescence signals diverge and the final fluorescence emitted by sample 9 equals that of sample 2, which contains 100-fold more target copies. However, the threshold cycle is determined much earlier (see graph c). This indicates that end-point fluorescence detection is not a valid method for quantitation.

values in synovial fluid samples from OA patients (Fig. 4A). Similar results were obtained for mRNA levels (Fig. 4B) by real-time RT-PCR. Therefore, in this model, increased mRNA levels as detected by real-time RT-PCR coincide with increased protein expression as determined by ELISA.

3.5. Change in cytokine and cytokine receptor levels during IL-10 therapy of patients with psoriasis

Before the initiation of IL-10 therapy, levels of TNFα, IFNγ, IL-8 and its receptor CXCR2 were

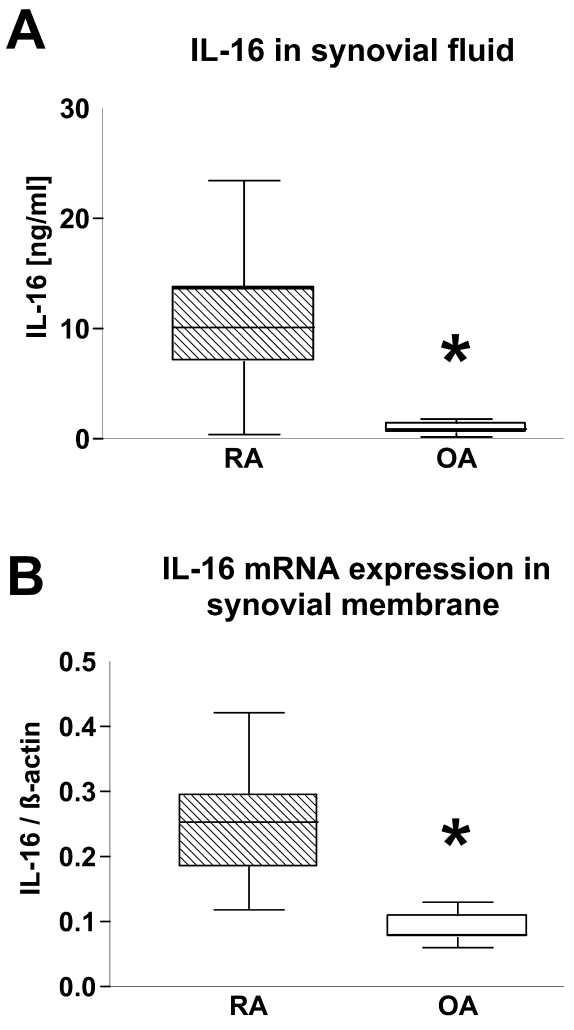

Fig. 4. IL-16 expression in rheumatoid arthritis. (A) IL-16 was quantified by ELISA in synovial fluid from patients with RA ($n=15$) and OA ($n=15$). (B) IL-16 mRNA expression was quantified in synovial membrane tissue (RA, $n=25$; OA, $n=10$) by real-time quantitative RT-PCR. Whiskers indicate data range, boxes extend from the 25–75th percentile and the horizontal lines indicate the median. Asterisks indicate significantly lower values in OA patients compared to RA patients ($P<0.05$).

markedly elevated in active psoriasis ($n=14$) when compared to normal skin ($n=5$), reflecting lesional inflammation. After 42 days of therapy, cutaneous levels of the proinflammatory cytokines and CXCR2 were significantly decreased (Fig. 5). This decrease was associated with a marked reduction in clinical disease severity as indicated by a decrease of the PASI score from 22.4 to 8.4 at the end of treatment ($P<0.0001$, Wilcoxon signed rank test, Reich et al., submitted). However, cytokine levels at the end of therapy remained above those detected in normal skin, and a complete remission of clinical symptoms was not observed in any of the treated patients.

4. Discussion

In this study, we have evaluated the use of real-time quantitative RT-PCR technology for the detection of cytokine gene expression in cultured cells and small tissue samples. The validity of the method was studied using different experimental applications of RT-PCR in cytokine analysis. First, the results obtained for IL-16 gene expression by real-time RT-PCR in monocyte-derived dendritic cells were compared to those obtained by the currently preferred method, quantitative competitive RT-PCR. Second, mRNA levels of cytokines determined by real-time RT-PCR in synovial tissue from arthritis patients were correlated with protein expression in synovial fluid. Third, the effect of immunomodulatory therapy on cytokine gene expression in psoriatic skin lesions as determined by real-time RT-PCR was compared with the decrease of clinical symptoms. Our results clearly show that real-time RT-PCR is a useful method for quantifying even low level cytokine gene expression.

RT-PCR has proven to be a useful tool to study mRNA expression in small amounts of tissue, e.g., for the study of cytokines in the pathogenesis of disease. Although it is possible to homogenize fresh material for the quantitation of cytokines in the supernatant (Beck et al., 1996), the tools (such as ELISA) are not sensitive and permit only a very limited number of analyses. Since biopsy material is often paraffin embedded or cryopreserved, ELISA determinations may not be possible. From cryopreserved material, mRNA can be extracted for Northern blot analysis, but more than 10 μg of total RNA may be needed for the detection of a single cytokine, which exceeds the yield from typical skin biopsies. Therefore, because of its high sensitivity, RT-PCR has increased in popularity. However, since target sequences are theoretically amplified some 2^{35}-fold, small variations in amplification efficiency may lead

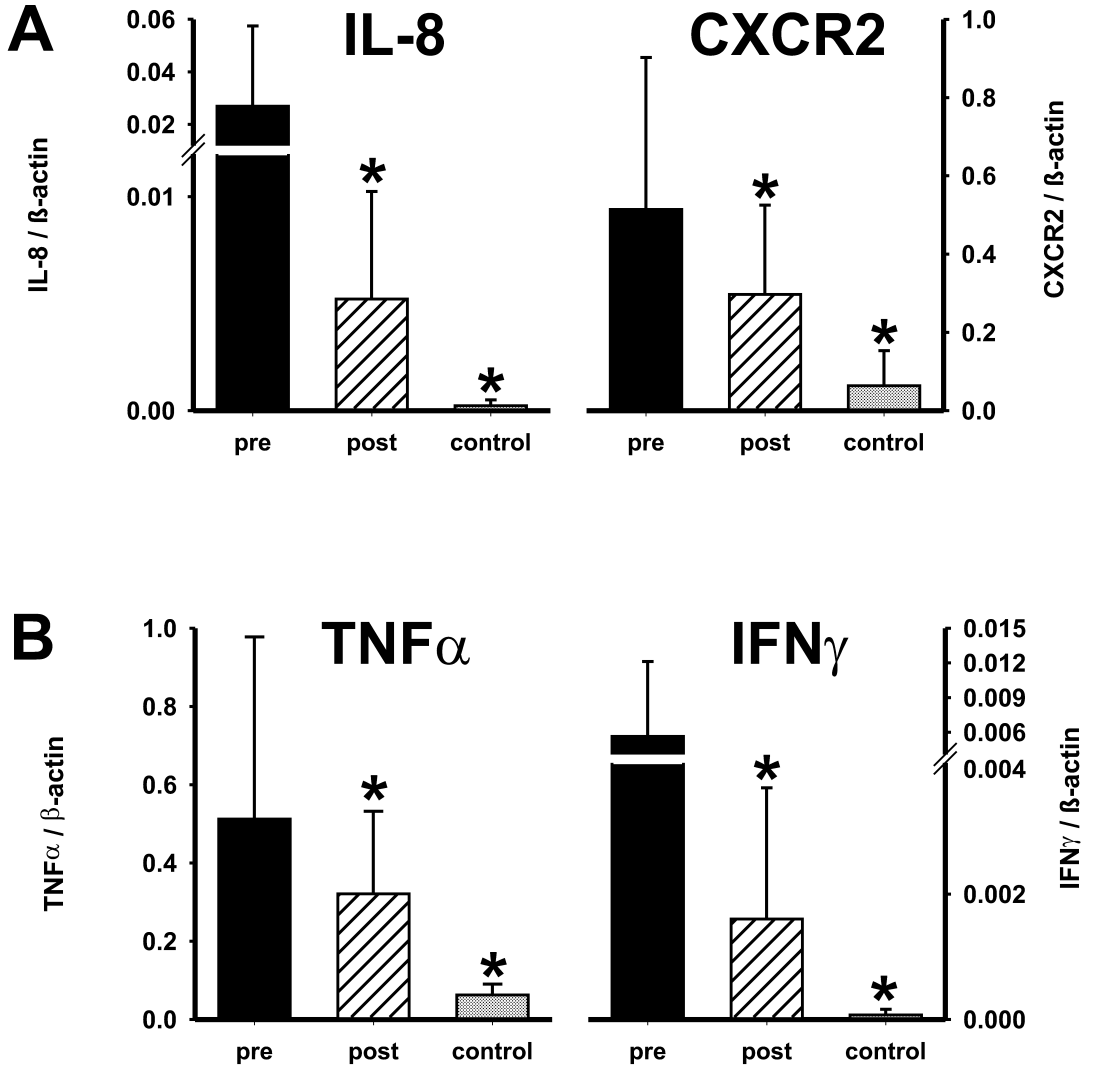

Fig. 5. Modulation of cytokine expression in psoriatic lesions by IL-10 therapy. Fourteen patients with chronic plaque psoriasis were treated subcutaneously with IL-10 for 42 days. Before and after therapy, cytokine expression within the marker lesion was quantified by real-time RT-PCR. (A) IL-8 and its receptor CXCR2. (B) TNFα and IFNγ. All post-treatment levels are significantly reduced as compared to pre-treatment levels, but still significantly elevated above normal skin (control). Mean±S.D., asterisks indicate significant inter-group differences for each cytokine and receptor ($P<0.05$).

to significant changes in PCR product yield (Gilliland et al., 1990). The reason for inter-sample variations of amplification efficiency are poorly understood, but inhomogeneous heat distribution within common thermal block cyclers might play an important role. It is therefore generally agreed that quantitation by simple PCR product densitometry is obsolete. With the introduction of internal standards into the amplification process, amplification efficiency can be monitored (Siegling et al., 1994). To compare different samples, variations between samples, e.g., during reverse transcription, need to be controlled by quantifying a housekeeping gene (e.g., β-actin, Platzer et al., 1992), which is assumed to be equally expressed in the investigated tissues. However, the generation and coamplification of internal

standards, which usually consist of shortened PCR fragments, is difficult and time consuming. Therefore, in an alternative approach, dilution series of the target product are prepared as external controls and used to generate calibration curves (Heid et al., 1996). In the absence of internal controls it is necessary that all samples are amplified with the same efficiency. While common thermal block cyclers may not be suitable in this case, cyclers providing a homogeneous thermal distribution, such as the hot-air vent cyclers, could overcome this problem. In fact, as described in this study using the LightCycler® system (Roche Diagnostics), the inter-sample variation in amplification efficiency was small as results obtained from duplicate samples typically differed by less than 10%.

Quantitation by LightCycler® real-time RT-PCR is based on the threshold cycle method. For each sample, a determination is made of the cycle number at which the fluorescence related to the amount of double-stranded DNA is significantly elevated above background fluorescence. The more specific transcripts that are present, the less cycles are necessary to generate a significant signal (Heid et al., 1996). By using external standards, a calibration curve can be generated and samples can be quantified according to their threshold cycle. When hot air is used to heat or cool sample tubes, e.g., glass capillaries in this system, the cycling and subsequent analytical process may take as little as 30 min as compared to several hours with conventional PCR cyclers and agarose gel electrophoresis. In contrast to the common gel electrophoretic bands, which indicate successful and specific amplification of the specific PCR product, the LightCyler® system provides a melting curve analysis of the PCR products. With optimized cycling parameters, only the specific PCR product is obtained, resulting in a single narrow melting peak, which correlates with a single band by gel electrophoresis. During subsequent real-time PCR reactions, PCR product identity can routinely be ascertained by a melting curve analysis. As with ordinary RT-PCR, primer-dimer formation also occurred during real-time RT-PCR. However, in each case it was possible to select a temperature at which primer-dimers had completely melted, but at which the specific PCR product was not affected. Importantly, by using this temperature during fluorescence detection, no signals were observed in negative control reactions. It is also noteworthy that because quantitation is performed early during PCR, it is independent of variations possibly occurring during late stages of the cycling process (compare Fig. 3). Analysis of the standard dilution series revealed that as little as 120 target copies could reliably be quantified with this method.

In this study, we used quantitative real-time RT-PCR to investigate the expression of IL-16, a chemoattractant specific for CD4-bearing cells. IL-16 is regarded as a proinflammatory cytokine since it has been shown to upregulate HLA-DR as well as CD25-expression (Parada et al., 1998). Recently identified cellular sources of IL-16 include T-cells, eosinophils and mast cells. In cutaneous inflammatory responses, e.g., in atopic and contact dermatitis, a strong $CD4^+$ infiltrate is observed. We therefore speculated that IL-16 might be involved in recruiting the infiltrate and sustaining the inflammatory response. We focused on monocyte-derived dendritic since these resemble cutaneous dendritic cells, the most important antigen-presenting cells in human skin. During maturation of monocyte-derived dendritic cells we observed a strong expression shortly after monocyte purification. After 2 days of culture, IL-16 gene expression was markedly reduced. Although cells were purified by positive CD14 selection, we cannot exclude contamination with lymphocytes and granulocytes. It is therefore likely that the high initial expression of IL-16, followed by a dramatic decrease during the following 2 days, originated from contaminating cells which rapidly disappeared from the cultures. During culture of dendritic cells IL-16 expression peaked in immature dendritic cells (day 5) and declined with maturation. A similar expression pattern has recently been shown for IL-12, another proinflammatory cytokine with strong effects on T-cells (Kalinski et al., 1999). The decreased production of cytokines such as IL-12 and IL-16 in vitro may correspond to a reduced cytokine release from dendritic cells migrating from skin to regional lymph nodes in vivo. Such a mechanism would limit the effects of dendritic cell-derived cytokines to the site of initial antigen challenge.

Secondly, we have investigated the role of IL-16 in rheumatoid arthritis. In contrast to osteoarthritis patients, a significant $CD4^+$ infiltrate is present in the affected joints of patients with rheumatoid arth-

ritis. In rheumatoid patients, elevated levels of IL-16 have been reported in the synovial fluid and the expression of IL-16 has been demonstrated by in situ hybridization in the synovial membrane (Franz et al., 1998). By real-time RT-PCR we found that IL-16 mRNA is expressed in lesional synovial membrane tissue at significantly higher levels than in OA. This observation was paralleled by the finding that in synovial fluid from RA patients IL-16 protein levels are significantly elevated when compared to OA patients. Therefore, it is possible that IL-16 could be involved in recruiting $CD4^+$ cells to affected joints in RA.

Finally, we have used real-time RT-PCR to identify disease-related genes in psoriasis and to monitor the expression of these genes during experimental IL-10 therapy. Psoriasis is a chronic inflammatory skin condition of unknown origin. Enhanced keratinocyte proliferation is thought to be driven by cytokines such as TNFα and IFNγ released from infiltrating Th-1 cells. Neutrophils are also abundant in affected skin and may be attracted by chemotactic factors such as IL-8 that acts via the chemokine receptors CXCR1 and 2. By quantitative real-time RT-PCR we confirmed the important role of Th-1 and IL-8/CXCR2 pathways in psoriasis and were able to demonstrate a significant overexpression in lesional compared to normal skin. During therapy, we found significant reductions in the gene expression of the proinflammatory cytokines as well as CXCR2, paralleled by a clearing of clinical symptoms. Recently, a study involving IL-11 therapy reported similar results (Trepicchio et al., 1999) using sequence-specific probes for real-time RT-PCR. However, sequence-specific probes are expensive and have to be individually designed. Here, we show that SYBR Green-based real-time RT-PCR, which does not require sequence-specific probes, is a valid method for quantifying even low-level cytokine gene expression.

Real-time PCR has been employed to quantify minimal residual disease in hematological malignancies as a measure of therapeutic efficacy (Cassinat et al., 2000; Eckert et al., 2000). It may also prove to be a reliable tool for the detection of early relapse. Monitoring residual circulating malignant cells with both quantitative competitive and real-time RT-PCR using sequence-specific hybridization probes (Emig et al., 1999; Wattjes et al., 2000) has demonstrated the applicability of the new method in this setting. The results of our study extend these findings and show that real-time RT-PCR is a rapid, reliable and valid method for the detection of cytokines and may be useful in various clinical applications, such as the identification of disease-related genes and pharmacogenomic monitoring. Since it is significantly less time consuming (30 min versus several hours) than the currently preferred method, quantitative competitive RT-PCR, it might become the method of choice within the near future.

Acknowledgements

We highly appreciate the skillful technical assistance of Ms. Karolin Zachmann and Mr. Thomas Juergens.

References

Beck, L.A., Stellato, C., Beall, L.D., Schall, T.J., Leopold, D., Bickel, C.A., Baroody, F., Bochner, B.S., Schleimer, R.P., 1996. Detection of the chemokine RANTES and endothelial adhesion molecules in nasal polyps. J. Allergy Clin. Immunol. 98, 766.

Blaschke, V., Jungermann, K., Püschel, G.P., 1996. Exclusive expression of the Gs-linked prostaglandin E2 receptor subtype 4 mRNA in mononuclear Jurkat and KM-3 cells and coexpression of subtype 4 and 2 mRNA in U-937 cells. FEBS Lett. 394, 39.

Blaschke, V., Reich, K., Middel, P., Letschert, M., Sachse, F., Harwix, S., Neumann, C., 1999. Expression of the CD4+ cell-specific chemoattractant interleukin-16 in mycosis fungoides. J. Invest. Dermatol. 113, 658.

Cassinat, B., Zassadowski, F., Balitrand, N., Barbey, C., Rain, J.D., Fenaux, P., Degos, L., Vidaud, M., Chomienne, C., 2000. Quantitation of minimal residual disease in acute promyelocytic leukemia patients with t(15;17) translocation using real time RT-PCR. Leukemia 14, 324.

Eckert, C., Landt, O., Taube, T., Seeger, K., Beyermann, B., Proba, J., Henze, G., 2000. Potential of LightCycler technology for quantification of minimal residual disease in childhood acute lymphoblastic leukemia. Leukemia 14, 316.

Emig, M., Saussele, S., Wittor, H., Weisser, A., Reiter, A., Willer, A., Berger, U., Hehlmann, R., Cross, N.C., Hochhaus, A., 1999. Accurate and rapid analysis of residual disease in patients with CML using specific fluorescent hybridization probes for real time quantitative RT-PCR. Leukemia 13, 1825.

Franz, J.K., Kolb, S.A., Hummel, K.M., Lahrtz, F., Neidhart, M.,

Aicher, W.K., Pap, T., Gay, R.E., Fontana, A., Gay, S., 1998. Interleukin-16, produced by synovial fibroblasts, mediates chemoattraction for $CD4^+$ T lymphocytes in rheumatoid arthritis. Eur. J. Immunol. 28, 2661.

Gilliland, G., Perrin, S., Blanchard, K., Bunn, H.F., 1990. Analysis of cytokine mRNA and DNA: detection and quantitation by competitive polymerase chain reaction. Proc. Natl. Acad. Sci. USA 87, 2725.

Heid, C.A., Stevens, J., Livak, K.J., Williams, P.M., 1996. Real time quantitative PCR. Genome Res. 6, 986.

Higuchi, R., Dollinger, G., Walsh, P.S., Griffith, R., 1992. Simultaneous amplification and detection of specific DNA sequences. Biotechnology (NY) 10, 413.

Kalinski, P., Schuitemaker, J.H., Hilkens, C.M., Wierenga, E.A., Kapsenberg, M.L., 1999. Final maturation of dendritic cells is associated with impaired responsiveness to IFN-gamma and to bacterial IL-12 inducers: decreased ability of mature dendritic cells to produce IL-12 during the interaction with Th cells. J. Immunol. 162, 3231.

Neumann, C., Gutgesell, C., Fliegert, F., Bonifer, R., Herrmann, F., 1996. Comparative analysis of the frequency of house dust mite specific and nonspecific Th1 and Th2 cells in skin lesions and peripheral blood of patients with atopic dermatitis. J. Mol. Med. 74, 401.

Palucka, K.A., Taquet, N., Sanchez-Chapuis, F., Gluckman, J.C., 1998. Dendritic cells as the terminal stage of monocyte differentiation. J. Immunol. 160, 4587.

Parada, N.A., Center, D.M., Kornfeld, H., Rodriguez, W.L., Cook, J., Vallen, M., Cruikshank, W.W., 1998. Synergistic activation of CD4+ T cells by IL-16 and IL-2. J. Immunol. 160, 2115.

Platzer, C., Richter, G., Uberla, K., Muller, W., Blocker, H., Diamantstein, T., Blankenstein, T., 1992. Analysis of cytokine mRNA levels in interleukin-4-transgenic mice by quantitative polymerase chain reaction. Eur. J. Immunol. 22, 1179.

Reich, K., Bruck, M., Gräfe, A., Vente, C., Neumann, C., Garbe, C., 1998. Treatment of psoriasis with interleukin-10. J. Invest. Dermatol. 111, 1235.

Reich, K., Westphal, G., Schulz, T., Müller, M., Zipprich, S., Fuchs, T., Hallier, E., Neumann, C., 1999. Combined analysis of polymorphisms of the tumor necrosis factor-alpha and interleukin-10 promoter regions and polymorphic xenobiotic metabolizing enzymes in psoriasis. J. Invest. Dermatol. 113, 214.

Romani, N., Reider, D., Heuer, M., Ebner, S., Kampgen, E., Eibl, B., Niederwieser, D., Schuler, G., 1996. Generation of mature dendritic cells from human blood. An improved method with special regard to clinical applicability. J. Immunol. Methods 196, 137.

Sager, N., Feldmann, A., Schilling, G., Kreitsch, P., Neumann, C., 1992. House dust mite-specific T cells in the skin of subjects with atopic dermatitis: frequency and lymphokine profile in the allergen patch test. J. Allergy Clin. Immunol. 89, 801.

Schlaak, J.F., Buslau, M., Jochum, W., Hermann, E., Girndt, M., Gallati, H., Meyer zum Büschenfelde, K.H., Fleischer, B., 1994. T cells involved in psoriasis vulgaris belong to the Th1 subset. J. Invest. Dermatol. 102, 145.

Siegling, A., Lehmann, M., Platzer, C., Emmrich, F., Volk, H.D., 1994. A novel multispecific competitor fragment for quantitative PCR analysis of cytokine gene expression in rats. J. Immunol. Methods 177, 23.

Trepicchio, W.L., Ozawa, M., Walters, I.B., Kikuchi, T., Gilleaudeau, P., Bliss, J.L., Schwertschlag, U., Dorner, A.J., Krueger, J.G., 1999. Interleukin-11 therapy selectively downregulates type I cytokine proinflammatory pathways in psoriasis lesions. J. Clin. Invest. 104, 1527.

Uyemura, K., Yamamura, M., Fivenson, D.F., Modlin, R.L., Nickoloff, B.J., 1993. The cytokine network in lesional and lesion-free psoriatic skin is characterized by a T-helper type 1 cell-mediated response. J. Invest. Dermatol. 101, 701.

Wattjes, M.P., Krauter, J., Nagel, S., Heidenreich, O., Ganser, A., Heil, G., 2000. Comparison of nested competitive RT-PCR and real time RT-PCR for the detection and quantification of AML1/MTG8 fusion transcripts in t(8;21) positive acute myelogenous leukemia. Leukemia 14, 329.